

# ZnO-coated $\text{LiMn}_2\text{O}_4$ cathode material for lithium-ion batteries synthesized by a combustion method

Qi-Ling Li<sup>1</sup> · Wang-Qiong Xu<sup>1,2</sup> · Hong-Li Bai<sup>1,2</sup> · Jun-Ming Guo<sup>1,2</sup> · Chang-Wei Su<sup>1,2</sup>

Received: 18 December 2015 / Revised: 15 January 2016 / Accepted: 18 January 2016 / Published online: 6 February 2016  
© Springer-Verlag Berlin Heidelberg 2016

**Abstract** ZnO-coated  $\text{LiMn}_2\text{O}_4$  cathode materials were prepared by a combustion method using glucose as fuel. The phase structures, size of particles, morphology, and electrochemical performance of pristine and ZnO-coated  $\text{LiMn}_2\text{O}_4$  powders are studied in detail by X-ray diffraction (XRD), scanning electron microscopy (SEM), transmission electron microscopy (TEM), cyclic voltammetry (CV), electrochemical impedance spectroscopy (EIS), galvanostatic charge-discharge test, and X-ray photoelectron spectroscopy (XPS). XRD patterns indicated that surface-modified ZnO have no obvious effect on the bulk structure of the  $\text{LiMn}_2\text{O}_4$ . TEM and XPS proved ZnO formation on the surface of the  $\text{LiMn}_2\text{O}_4$  particles. Galvanostatic charge/discharge test and rate performance showed that the ZnO coating could improve the capacity and cycling performance of  $\text{LiMn}_2\text{O}_4$ . The 2 wt% ZnO-coated  $\text{LiMn}_2\text{O}_4$  sample exhibited an initial discharge capacity of  $112.8 \text{ mAh g}^{-1}$  with a capacity retention of 84.1 % after 500 cycles at 0.5 C. Besides, a good rate capability at different current densities from 0.5 to 5.0 C can be acquired. CV and EIS measurements showed that the ZnO coating effectively reduced the impacts of polarization and charge transfer resistance upon cycling.

**Keywords** Spinel  $\text{LiMn}_2\text{O}_4$  · ZnO-coated  $\text{LiMn}_2\text{O}_4$  · Combustion method · Lithium ion batteries · Cathode materials

## Introduction

Nowadays, the development of lithium-ion batteries with high power density and high energy density has been accelerated due to the trend of miniaturization of portable electronic devices as well as the development of electric vehicles. At this time, layered  $\text{LiMO}_2$  ( $M = \text{Mn, Co, Ni}$ ),  $\text{LiNi}_{0.3}\text{Mn}_{0.3}\text{Co}_{0.3}\text{O}_2$ , olivine-type  $\text{LiFePO}_4$ , spinel-type  $\text{LiMn}_2\text{O}_4$ , lithium-rich material  $x\text{Li}_2\text{MnO}_3 \cdot (1-x)\text{LiMO}_2$  ( $M = \text{Co, Fe, Ni}_{1/2}\text{Mn}_{1/2}$ ), etc. are the main cathode materials for rechargeable lithium-ion batteries. Among the various choices of cathode materials, the spinel lithium manganese oxide ( $\text{LiMn}_2\text{O}_4$ ) is considered to be one of the promising cathode materials for lithium-ion batteries due to its advantages such as the abundance of raw materials, cheap resources, and environment friendliness. So it has been extensively considered as an alternative positive electrode material [1–4]. Nevertheless, the capacity fading of  $\text{LiMn}_2\text{O}_4$  is a deadly obstacle which limits its commercial use. The reasons for fast capacity fading have been investigated, and they were mainly ascribed to the following three factors: (I) the dissolution of manganese into an electrolyte during cycling [5, 6], (II) Jahn-Teller distortion [7], and (III) the decomposition of the electrolyte solution [8].

There are two kinds of strategies to overcome the aforementioned problems. One way is substitution of heterogeneous atoms into the host spinel  $\text{LiMn}_2\text{O}_4$  structure to improve the structural stability. This strategy, however, reduces the initial discharge capacity. The other one is surface modification. Coating the cathode material with various particles or films including  $\text{SiO}_2$ , ZnO,  $\text{CeO}_2$ ,  $\text{LaF}_3$ ,  $\text{FePO}_4$ , etc. can

✉ Jun-Ming Guo  
guojunming@tsinghua.org.cn

<sup>1</sup> Key Laboratory of Comprehensive Utilization of Mineral Resources in Ethnic Regions, School of Chemistry and Environment, Yunnan Minzu University, Kunming 650500, People's Republic of China

<sup>2</sup> Key Laboratory of Resource Clean Conversion in Ethnic Regions, Education Department of Yunnan, School of Chemistry and Environment, Yunnan Minzu University, Kunming 650500, People's Republic of China

effectively minimize the direct contact area between the  $\text{LiMn}_2\text{O}_4$  electrode and electrolyte and further inhibit the Mn dissolution during the cycling process [9–13]. Researches showed that surface modification techniques and the types of coating materials can affect the characteristics of electrode materials [14, 15]. Nowadays, most surface modification approaches of spinel lithium manganese oxide reported in the literature are carried out with sol-gel method [10], chemical deposition method [16], precipitation method [17], polymeric process [18], melting impregnation method [19], atomic layer deposition (ALD) method [20], and so on. ZnO was regarded as a desirable surface-coating material due to its excellent chemical and thermal stability. Some studies of ZnO-coated  $\text{LiFePO}_4$ ,  $\text{LiMn}_{1.5}\text{Ni}_{0.5}\text{O}_4$ ,  $\text{LiNi}_{0.5}\text{Co}_{0.2}\text{Mn}_{0.3}\text{O}_2$ , and  $\text{LiMn}_2\text{O}_4$  have been reported by using different coating techniques to improve their electrochemical performance [21–25]. Tu et al. [15] coated ZnO on  $\text{LiMn}_2\text{O}_4$  particles via the melting impregnation method. The ZnO coating sample showed a capacity retention rate of 96.36 % at 0.5 C after 100 cycles. Liu et al. [10] reported ZnO-coated  $\text{LiMn}_2\text{O}_4$  by the sol-gel method. The 2 wt% ZnO-coated  $\text{LiMn}_2\text{O}_4$  delivered an average capacity loss of 0.19 % per cycle in 50 cycles under a current rate of 0.5 C. Recently, Zhao et al. [20] used the ALD method to deposit ultrathin and highly conformal ZnO coatings onto  $\text{LiMn}_2\text{O}_4$  cathodes. They have obtained a better cycling performance compared to the pristine  $\text{LiMn}_2\text{O}_4$ . However, to the best of our knowledge, there are no reports on ZnO-coated  $\text{LiMn}_2\text{O}_4$  cathode materials prepared by a combustion method so far.

In our previous paper, we have successfully synthesized a single phase of spinel  $\text{LiMn}_2\text{O}_4$  powders using a combustion method [26]. However, the  $\text{LiMn}_2\text{O}_4$  did not achieve the desired capacity retention. In this paper, ZnO was selected for coating over the surface of  $\text{LiMn}_2\text{O}_4$  cathodes to further improve their capacity and cycling performance. The effects of coating on the structure, morphology, and electrochemical performance of cathode materials are investigated in detail.

## Experimental

### Sample preparation

#### *Synthesis of $\text{LiMn}_2\text{O}_4$ powders*

The synthesis method of  $\text{LiMn}_2\text{O}_4$  was referred to the literature [26]. Stoichiometric amounts of lithium nitrate ( $\text{LiNO}_3$ , AR, aladdin) and manganese acetate ( $\text{Mn}(\text{CH}_3\text{COO})_2 \cdot 4\text{H}_2\text{O}$ , AR, aladdin) were dissolved in 9 mol  $\text{L}^{-1}$  nitric acid and then placed in a 300-mL crucible. The mixture was calcined at 600 °C for 3 h in a muffle; then, the product was taken out and cooled down to room temperature naturally to get  $\text{LiMn}_2\text{O}_4$  powders.

#### *Synthesis of ZnO and ZnO-coated $\text{LiMn}_2\text{O}_4$ powders*

ZnO-coated  $\text{LiMn}_2\text{O}_4$  cathode materials were synthesized using glucose as fuel by a combustion method. Firstly, zinc acetate ( $\text{Zn}(\text{CH}_3\text{COO})_2 \cdot 2\text{H}_2\text{O}$ ) (AR, Tianjin, China Chemical Co., Ltd.) was dissolved in a water medium, and glucose (10 wt%) was added into the solution followed by continuous stirring for 15 min. Subsequently, previously synthesized  $\text{LiMn}_2\text{O}_4$  powders were dispersed into the mixture. The mixture was stirred for 1 h to form a homogeneously dispersed suspension. The precursor was dried and calcined at 500 °C for 3 h to obtain the ZnO-coated  $\text{LiMn}_2\text{O}_4$ . The expected amounts of the ZnO coating are 1, 2, and 5 wt% of the total  $\text{LiMn}_2\text{O}_4$  powder weight, respectively.

In order to investigate the crystal structure of ZnO, the powder of ZnO was prepared via thermal decomposition of zinc acetate. Firstly, zinc acetate was dispersed in the water medium, and then glucose (10 wt%) was added into the solution. The mixture was stirred for 1 h to obtain a homogeneously dispersed suspension. The precursor was dried and calcined at 500 °C for 3 h to obtain the ZnO powders.

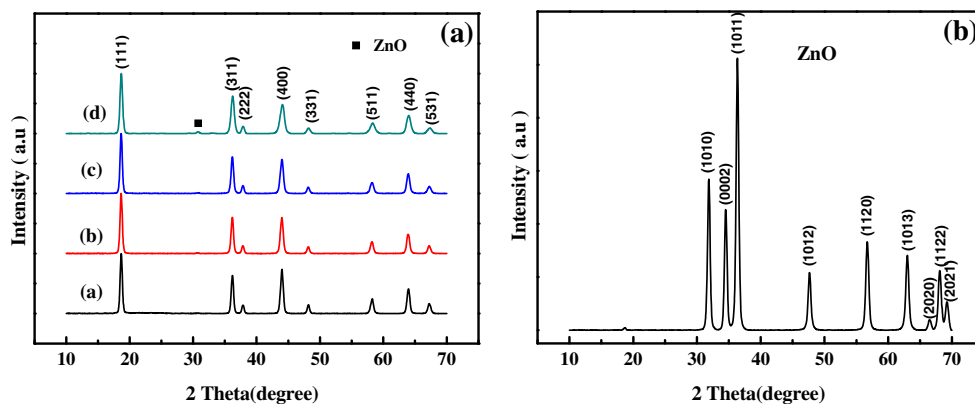
### Characterization of ZnO-coated $\text{LiMn}_2\text{O}_4$ cathode materials

The phase identification of the samples is performed on a diffractometer (X-ray diffraction (XRD), D/Max-TTRIII, Japan) using  $\text{Cu K}\alpha$  radiation; the scanning range of diffraction angle (2-theta) is 10°–70°. The scanning rate was 4°  $\text{min}^{-1}$  and the step width was 0.02° with 30 mA operation current and 40 kV voltage. The lattice parameters of the samples are calculated by using MDI Jade software. The morphology of the samples was observed by a scanning electron microscope (SEM, QUANTA 200, America FEI) equipped with an energy-dispersive spectrometer (EDS) and a transmission electron microscope (TEM, JEM-2100, JEOL). The value of *d*-spacing is measured by DigitalMicrograph software. X-ray photoelectron spectroscopy (XPS, PHI 5000 Versaprobe II, ULVAC-PHI, Japan) using monochromatic  $\text{Al K}\alpha$  (1486.6 eV) radiation was used to analyze chemical valence states of the samples, and the C 1s XPS binding energy at 284.6 eV was used as a calibration of the spectra.

### Electrochemical measurements

Electrochemical properties of as-prepared powders were measured with CR-2025 coin-type cells. The electrodes were fabricated by mixing the active materials of the powder, super P carbon black as a conductive, and polyvinylidene fluoride (PVDF) as a binder in a weight ratio of 8:1:1 in *N*-methylpyrrolidinone solvent. Then, the mixture was spread onto an aluminum current collector

**Fig. 1** XRD patterns of **a** the pristine  $\text{LiMn}_2\text{O}_4$  and various wt% ZnO-coated  $\text{LiMn}_2\text{O}_4$ : the (a) pristine, (b) 1 wt%, (c) 2 wt%, and (d) 5 wt% ZnO-coated  $\text{LiMn}_2\text{O}_4$  cathode materials. **b** XRD patterns of ZnO



and vacuum-dried at 120 °C for 10 h. The cells consisted of the as-fabricated electrodes as the positive electrode, metallic lithium as the counter electrode, a polypropylene film (Celgard 2320) as the separator, and the electrolyte 1 mol/L  $\text{LiPF}_6$  in EC and DEC (1:1 v/v). Cells were fabricated in an argon-filled glove box. The charge-discharge tests, cyclic performance, and rate performance tests were examined using a LAND battery program control cell tester (Wuhan Land Electronics Co., Ltd, China) between 3.0 and 4.5 V (vs.  $\text{Li/Li}^+$ ) at room temperature. Cyclic voltammetry (CV) was performed on a CHI604E electrochemical workstation (Shanghai Chenhua Instruments Co., Ltd, China) using a standard three-compartment cell in the potential range of 3.6–4.5 V and at a scan rate of  $0.05 \text{ mV s}^{-1}$  (vs.  $\text{Li/Li}^+$ ). Electrochemical impedance spectroscopy (EIS) spectra of cells were measured using the same electrochemical workstation in a frequency range of 0.1 Hz to 100 KHz with the applied AC signal amplitude of 10 mV.

## Results and discussion

### Characterization of the coating structures and morphology

Figure 1a shows the XRD patterns for un-coated  $\text{LiMn}_2\text{O}_4$  and ZnO-coated (1, 2, and 5 wt%)  $\text{LiMn}_2\text{O}_4$  powders, respectively. As expected in Fig. 1a, all the diffraction peaks could be indexed in a spinel structure of  $\text{LiMn}_2\text{O}_4$  (JCPDS card no. 35-0782) with a space group of  $Fd\bar{3}m$ , corresponding to the eight crystal planes of (111), (311), (222), (400), (331), (511), (440), and (531), where Li ions occupy tetrahedral sites (8a), Mn atoms octahedral sites (16d), and  $\text{O}^{2-}$  ions octahedral sites (32e) [27]. No impurity phase can be found in Fig. 1a(a–c). While the ZnO peak was detected in Fig. 1(d), no diffraction peaks from ZnO are observed in Fig. 1a(a–c), suggesting that the content of ZnO may be too low to be detected.

Compared with the un-coated  $\text{LiMn}_2\text{O}_4$ , 1 wt% ZnO-coated  $\text{LiMn}_2\text{O}_4$ , and 2 wt% ZnO-coated  $\text{LiMn}_2\text{O}_4$ , the 5 wt% ZnO-coated  $\text{LiMn}_2\text{O}_4$  sample obviously displays a broadening of FWHMs, indicating that the density of stacking faults increased after ZnO was surface-modified to a certain extent. This result was similar to an earlier report [19]. The lattice parameters are summarized in Table 1. The lattice constants of the coated materials compared with that of the un-coated  $\text{LiMn}_2\text{O}_4$  show no obvious change. Arumugam et al. [28] showed that the lattice parameter of samples increased with an increase in the amount of the dopant Zn. This indicated that ZnO coating does not change the structure of  $\text{LiMn}_2\text{O}_4$  and ZnO is just coated on the surface of  $\text{LiMn}_2\text{O}_4$  particles.

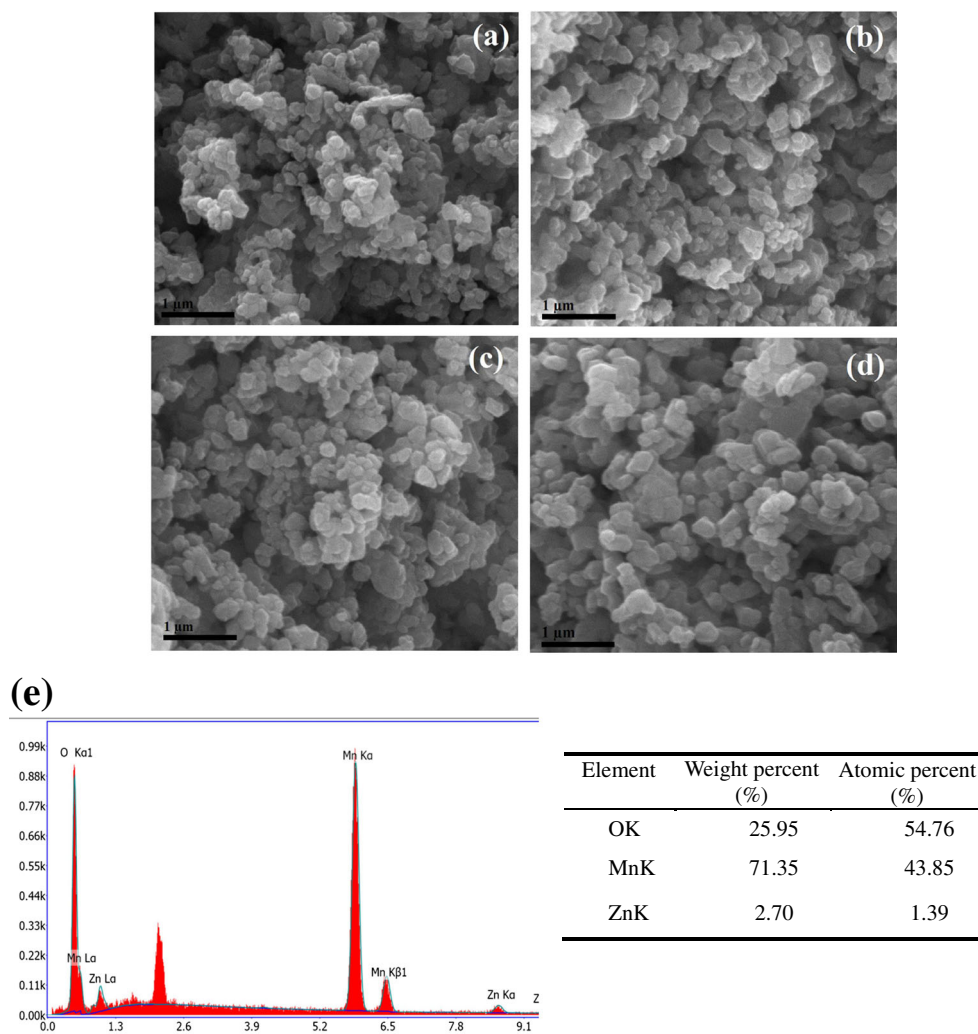
Figure 1b shows the XRD patterns of ZnO; all the diffraction peaks could be indexed with a wurtzite hexagonal structure of the bulk ZnO (JCPDS card no. 36-1451) confirmed by the peaks at  $31.8^\circ$ ,  $34.5^\circ$ , and  $36.3^\circ$  and correspond to the (1010), (0002), and (1011) planes of ZnO, respectively. And no impurity phases were observed in the spectrum, indicating that the pure ZnO powders are obtained via thermal decomposition of zinc acetate and the synthesized powder is single crystalline.

Figure 2a–d shows the SEM images of un-coated  $\text{LiMn}_2\text{O}_4$  and ZnO-coated (1, 2, and 5 wt%)  $\text{LiMn}_2\text{O}_4$  powders, respectively. The inset is the EDS profile of the 2 wt% ZnO-coated  $\text{LiMn}_2\text{O}_4$  sample. All the materials display agglomeration and irregular-shaped particles. The particle size increased from around 0.2 to 0.4  $\mu\text{m}$  as the ZnO coating content. It demonstrates that a small layer of ZnO coated on the surface of the

**Table 1** Lattice parameters of the pristine  $\text{LiMn}_2\text{O}_4$  and various wt% ZnO-coated  $\text{LiMn}_2\text{O}_4$  cathode materials

Sample	Pristine	1 wt% coated	2 wt% coated	5 wt% coated
Lattice parameters (Å)	8.239	8.237	8.239	8.232

**Fig. 2** The SEM images of pristine  $\text{LiMn}_2\text{O}_4$  and various wt% ZnO-coated  $\text{LiMn}_2\text{O}_4$ : the **a** pristine, **b** 1 wt%, **c** 2 wt%, and **d** 5 wt% ZnO-coated  $\text{LiMn}_2\text{O}_4$  cathode materials and the **e** EDS spectrum of the 2 wt% ZnO-coated  $\text{LiMn}_2\text{O}_4$  sample and the element content of the powder



$\text{LiMn}_2\text{O}_4$  enlarges the particle size of the pristine  $\text{LiMn}_2\text{O}_4$ . Zinc, manganese, and oxygen can be clearly observed in the EDS profile (Fig. 2e). The existence of Zn suggests that ZnO may deposit onto the particle surface of  $\text{LiMn}_2\text{O}_4$ .

TEM is used to further research the surface morphology of the bare  $\text{LiMn}_2\text{O}_4$  and ZnO-coated  $\text{LiMn}_2\text{O}_4$ . Figure 3a shows the TEM images of the un-coated  $\text{LiMn}_2\text{O}_4$  materials with a measured  $d$ -spacing value of

0.48 nm, corresponding to the (111) crystalline plane and possessing a smooth surface. Figure 3b shows the image of the 5 wt% ZnO-coated  $\text{LiMn}_2\text{O}_4$  cathode material. This image indicates that a physically distinct phase is attached to the  $\text{LiMn}_2\text{O}_4$  surface, which is a distinctly different surface structure compared with the pristine  $\text{LiMn}_2\text{O}_4$  sample, and the particles have a lattice spacing close to 0.51 nm, corresponding to the (0001) crystal

**Fig. 3** The TEM images of **a** pristine  $\text{LiMn}_2\text{O}_4$  and **b** 5 wt% ZnO-coated  $\text{LiMn}_2\text{O}_4$

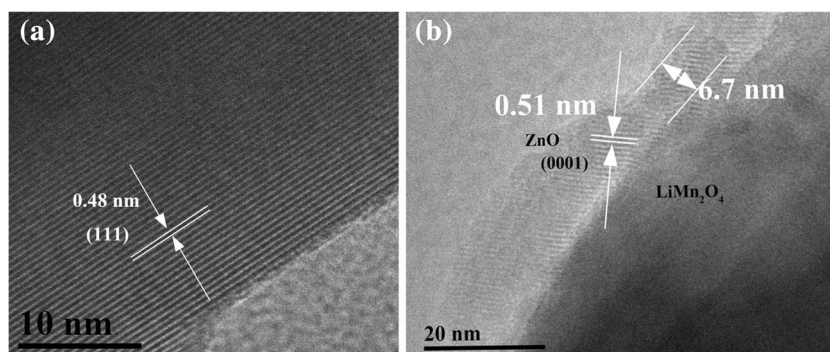
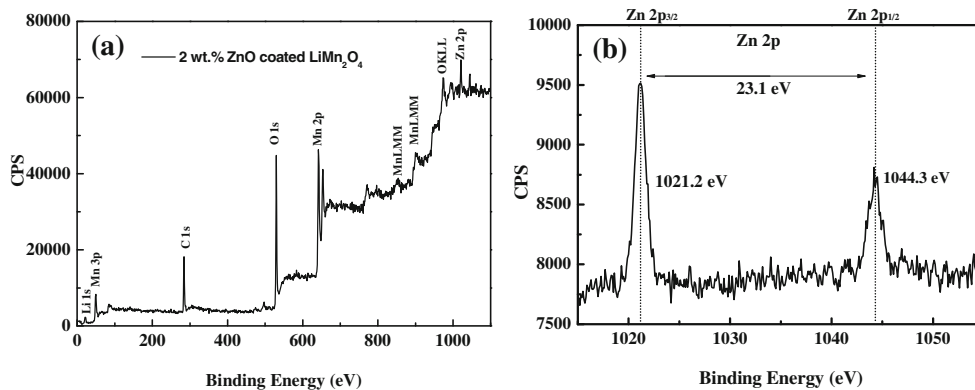




**Fig. 4** **a** XPS spectra of 2 wt% ZnO-coated LiMn<sub>2</sub>O<sub>4</sub> and **b** XPS spectra of Zn 2p



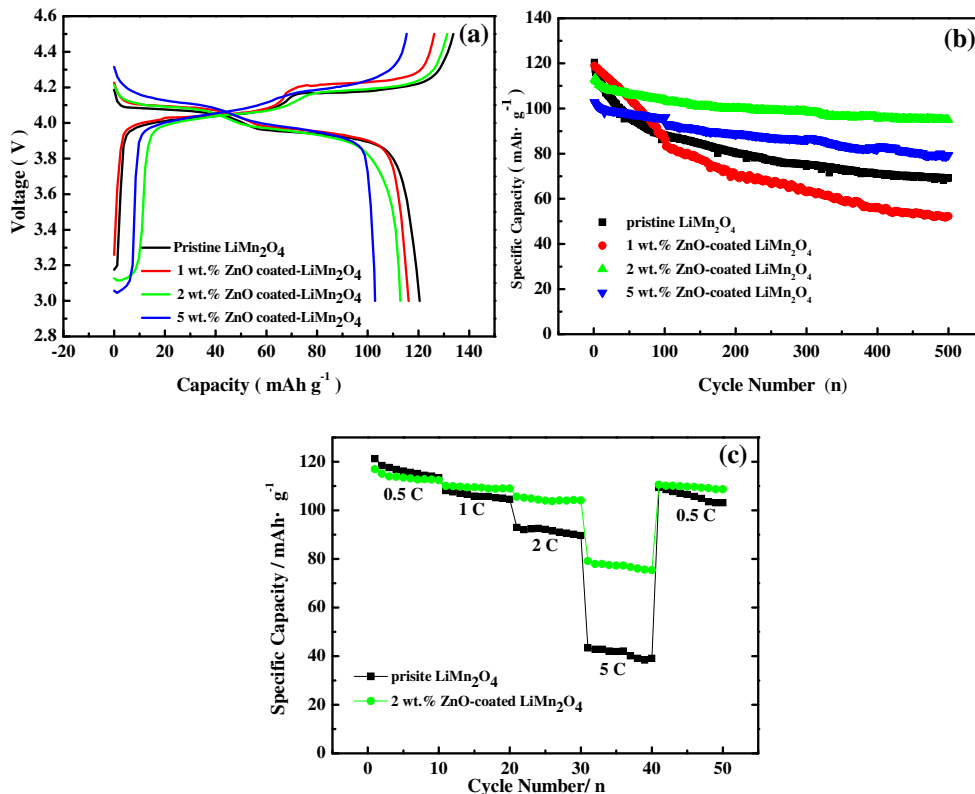
planes of the wurtzite ZnO [29, 30]. A uniform ZnO coating formed over the un-coated LiMn<sub>2</sub>O<sub>4</sub> particles with a coating layer with about 6.7 nm thickness, indicating that the oxide ZnO coating layer is crystalline, which is consistent with the XRD result.

XPS measurement was performed to examine surface compositions of the ZnO-coated LiMn<sub>2</sub>O<sub>4</sub> samples. As shown in Fig. 4a, the signals of Li, Mn, O, and Zn can be observed in the spectrum. In the Zn 2p spectrum (Fig. 4b), Zn 2p<sub>3/2</sub> and 2p<sub>1/2</sub> peaks at about 1021.2 and 1044.3 eV with a binding energy difference of 23.1 eV can be assigned to Zn(II), which is consistent with the reported papers on ZnO [31], which indicates a thin layer of ZnO forms on the surface of the LiMn<sub>2</sub>O<sub>4</sub> particles.

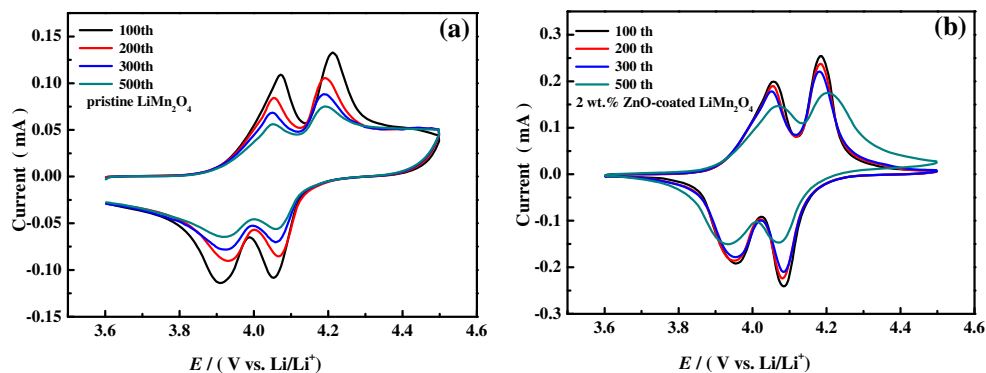
**Improvement in the cycling and rate performance of the spinel cathode**

Figure 5 shows the (a) initial charge-discharge and (b) cycling performance profiles of the un-coated and various wt% ZnO-coated LiMn<sub>2</sub>O<sub>4</sub> electrodes at 0.5 C (1 C = 148 mA g<sup>-1</sup>) between 3.0 and 4.5 V. As can be seen from the discharge profiles, the samples with two plateaus at around 4.05/4.20 V in the charge curve and at 3.9/4.1 V in the discharge curve indicate the two-step insertion/extraction reaction for the spinel LiMn<sub>2</sub>O<sub>4</sub>, which also corresponds to redox peaks in the CV curves (Fig. 6) [32]. The initial discharge capacities of the 1, 2,

**Fig. 5** **a** Initial charge-discharge curves of pristine LiMn<sub>2</sub>O<sub>4</sub> and various wt% ZnO-coated LiMn<sub>2</sub>O<sub>4</sub>. **b** Cycling performance curves of pristine LiMn<sub>2</sub>O<sub>4</sub> and various wt% ZnO-coated LiMn<sub>2</sub>O<sub>4</sub>, after 500 cycles at 0.5 C. **c** Rate performance of pristine LiMn<sub>2</sub>O<sub>4</sub> and 2 wt% ZnO-coated LiMn<sub>2</sub>O<sub>4</sub> from 0.5 to 5 C



**Fig. 6** Cyclic voltammogram curves of the 100th, 200th, 300th, and 500th cycles for the **a** pristine  $\text{LiMn}_2\text{O}_4$  and **b** 2 wt% ZnO-coated  $\text{LiMn}_2\text{O}_4$  samples are tested at a scan rate of  $0.05 \text{ mV s}^{-1}$  between 3.60 and 4.50 V



and 5 wt% ZnO-coated  $\text{LiMn}_2\text{O}_4$  were 116.1, 112.8, and 102.9  $\text{mAh g}^{-1}$ , respectively. Whereas that of the bare  $\text{LiMn}_2\text{O}_4$  fades from 120.4 to 69.2  $\text{mAh g}^{-1}$  after 500 cycles, 57.5 % of the original capacity is only reserved. However, the capacity retentions are 62.8 % for 1 wt%, 84.1 % for 2 wt%, and 77.1 % for 5 wt% ZnO after 500 cycles, respectively. Based on the above analysis, the 2 wt% ZnO-coated  $\text{LiMn}_2\text{O}_4$  sample is the optimum composition to enhance the stability and cycling performances of  $\text{LiMn}_2\text{O}_4$ ; as ZnO increases beyond the optimal coating content, the lower capacity retention and discharge capacity of composite electrodes may be ascribed to the blocking of lithium ion transport through a slightly thicker coating layer (herein ZnO), which results in more polarization rather than an electrochemical enhancement from the increased electronic conductivity [33]. It means that the fading in capacity suppression is due to modification with ZnO, which may minimize the surface area to suppress the side reactions between electrolyte solutions and cathode materials and to further inhibit the Mn dissolution

by the generation of acids such as HF during the cycling process [34].

Figure 5c displays the rate performance of un-coated  $\text{LiMn}_2\text{O}_4$  and 2 wt% ZnO-coated  $\text{LiMn}_2\text{O}_4$  from 0.5 to 5 C in the voltage range of 3.0–4.5 V. It can be observed that the discharge-specific capacity all decreases with the increasing rate due to electrochemistry polarization. The sample of  $\text{LiMn}_2\text{O}_4/2 \text{ wt% ZnO}$  possessed the highest discharge capacity of the electrodes at 5 C of  $79.1 \text{ mAh g}^{-1}$ , while the pristine  $\text{LiMn}_2\text{O}_4$  was only  $43.4 \text{ mAh g}^{-1}$  at the same condition. The cycling performance of 2 wt% ZnO-coated  $\text{LiMn}_2\text{O}_4$  is better than the ZnO-coated  $\text{LiMn}_2\text{O}_4$  samples prepared by ALD, because the ZnO-coated  $\text{LiMn}_2\text{O}_4$  samples prepared by atomic layer deposition delivers a capacity retention of 76 % after 100 cycles in 1 C at 25 °C and delivers a relatively low initial capacity ( $65.1 \text{ mAh g}^{-1}$ ) in 1 C [14]. However, the 2 wt% ZnO-coated  $\text{LiMn}_2\text{O}_4$  sample prepared by this combustion method delivers  $79.1 \text{ mAh g}^{-1}$  at a big current rate (5 C). Therefore, it is proposed that 2.0 wt% ZnO

**Fig. 7** Nyquist plots of the **a** pristine  $\text{LiMn}_2\text{O}_4$  and **b** 2 wt% ZnO-coated  $\text{LiMn}_2\text{O}_4$  samples investigated at the 100th, the 200th, the 300th, and the 500th cycles at room temperature. **c** The corresponding equivalent circuit

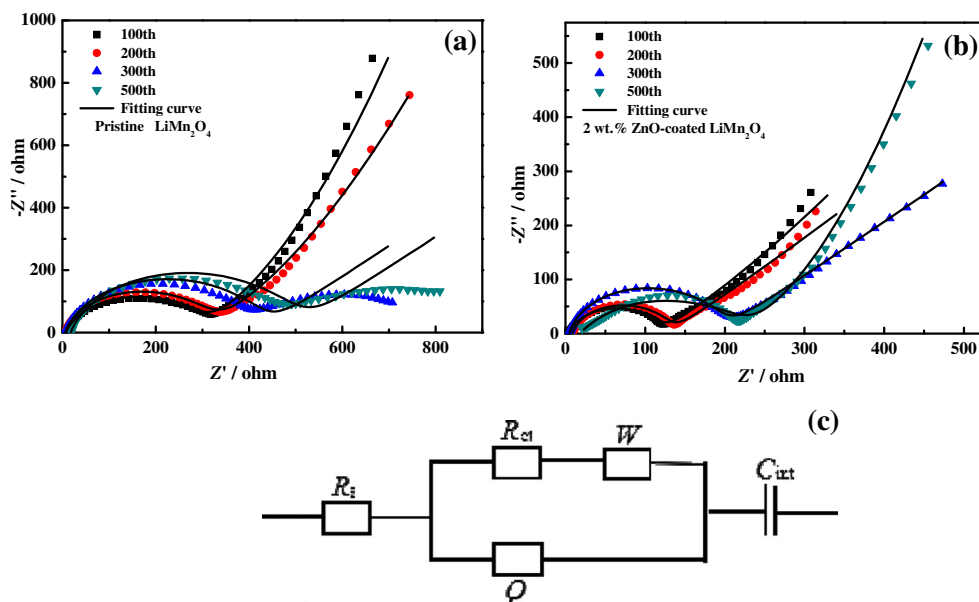


**Table 2** The fitting values of EIS at different cycles

Parameters	$R_s$ ( $\Omega$ )		$R_{ct}$ ( $\Omega$ )	
	Pristine	2 wt% ZnO-coated	Pristine	2 wt% ZnO-coated
At the 100th cycle	7.554	4.348	288.3	114.7
At the 200th cycle	6.504	8.98	306.6	121.3
At the 300th cycle	6.612	5.139	419.7	189.6
At the 500th cycle	17.75	4.786	480.9	208.6

coating is an outstandingly effective way for improving the rate capability of  $\text{LiMn}_2\text{O}_4$ .

### Cyclic voltammetric and electrochemical impedance spectroscopic behaviors of un-coated $\text{LiMn}_2\text{O}_4$ and 2 wt% ZnO-coated $\text{LiMn}_2\text{O}_4$

To further investigate the effect of ZnO coating on the mechanism of spinel  $\text{LiMn}_2\text{O}_4$ , cyclic voltammetry tests are conducted on the pristine  $\text{LiMn}_2\text{O}_4$  and 2.0 wt% ZnO-coated sample. Figure 6 shows the cyclic voltammogram curves of the 100th, 200th, 300th, and 500th cycles for the un-coated  $\text{LiMn}_2\text{O}_4$  and 2 wt% ZnO-coated  $\text{LiMn}_2\text{O}_4$  samples tested at a scan rate of  $0.05 \text{ mV s}^{-1}$  between 3.60 and 4.50 V. Two pairs of clear oxidation/reduction peaks can be observed from the CV curves associated with the typical two-step reversible intercalation/deintercalation of  $\text{Li}^+$  in spinel  $\text{LiMn}_2\text{O}_4$  [35], which shows good agreement with the corresponding two potential plateaus of the initial discharge curves from Fig. 5a discussed above. The peak currents of the un-coated  $\text{LiMn}_2\text{O}_4$  sample significantly decreases with the increasing charge-discharge cycling. However, the cyclic voltammogram curves present in Fig. 6b of the 2 wt% ZnO-coated  $\text{LiMn}_2\text{O}_4$  sample shows a distinct difference. With increasing of the charge-discharge cycling, the corresponding peak currents only incur a minor decrease before the 300th cycle. These results indicated that ZnO coating on the surface of  $\text{LiMn}_2\text{O}_4$  is an effective way to improve the electrochemistry performance, which corresponds to the good cycling performance of the ZnO-coated  $\text{LiMn}_2\text{O}_4$  sample shown in Fig. 5.

To clarify the effect of the ZnO coating on the electrochemical properties of  $\text{LiMn}_2\text{O}_4$ , Fig. 7 shows the Nyquist plots of (a) the un-coated  $\text{LiMn}_2\text{O}_4$  and (b) the 2 wt% ZnO-coated  $\text{LiMn}_2\text{O}_4$  samples investigated at different cycles at room temperature. The EIS of pristine  $\text{LiMn}_2\text{O}_4$  and 2 wt% ZnO-coated  $\text{LiMn}_2\text{O}_4$  are fitted by the ZSimpWin analysis software, and the EIS are simulated using the equivalent circuit shown in the inset of Fig. 7c. The values of parameters are listed in Table 2. A small interruption at the ( $Z'$ re) axis in the high-frequency region is assigned to the solution resistance ( $R_s$ ), the semicircle in the middle-frequency region is assigned to the charge transfer resistance ( $R_{ct}$ ) at the

interfacial capacitance between the electrolyte and electrodes [36], and the short line in the low-frequency region is caused by the diffusion of  $\text{Li}^+$  and is named Warburg impedance ( $W$ ) [37].  $C_{\text{int}}$  is the reflection of intercalation capacitance [38]. The constant phase element ( $Q$ ) represents the capacitance of the double layer. The  $R_{ct}$  of both samples increases with charge-discharge cycling. The  $R_{ct}$  of un-coated  $\text{LiMn}_2\text{O}_4$  increases from 288.3 to 480.9  $\Omega$ , and the  $R_{ct}$  of 2 wt% ZnO-coated  $\text{LiMn}_2\text{O}_4$  only increases from 114.7 to 208.6  $\Omega$ . Obviously, surface modification by coating ZnO can retard the increase of charge transfer resistance during the cycling test. A smaller  $R_{ct}$  is conducive for the electrochemical reaction of lithiation/delithiation, and the surface modification by coating ZnO guarantees a better cycling behavior than the pristine sample [39, 40], which agrees well with the electrochemical test results.

### XRD test after cycling

To further compare the crystal structure of 2 wt% ZnO-coated  $\text{LiMn}_2\text{O}_4$  before cycling and after 500 charge-discharge cycles, XRD was performed on the un-cycled and cycled electrodes for 500 cycles at 0.5 C as shown in Fig. 8. A small

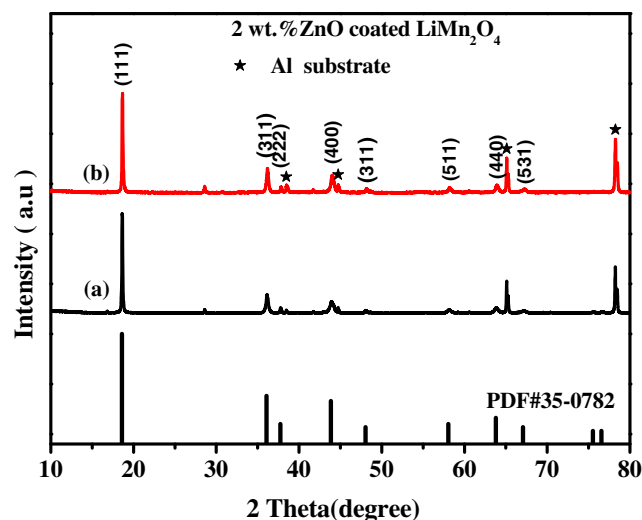


**Fig. 8** XRD patterns of 2 wt% ZnO-coated  $\text{LiMn}_2\text{O}_4$  a before cycling and b after 500 charge-discharge cycles at 0.5 C between 3.0 and 4.5 V at room temperature

amount of an impurity phase is detected in the XRD patterns (2-theta = 28.6°), because the working electrode includes 80 wt% active materials, 10 wt% super P carbon black, and 10 wt% PVDF. It can be seen that the powder also maintains a spinel  $\text{LiMn}_2\text{O}_4$  structure after 500 charge-discharge cycles, implying that ZnO coating can improve the structural stability of  $\text{LiMn}_2\text{O}_4$  during cycling, retard the side reactions between the electrode and electrolyte, further minimize the Mn dissolution during the cycling process, and result in a better cyclability and rate capability.

## Conclusions

ZnO-coated  $\text{LiMn}_2\text{O}_4$  was successfully synthesized by a combustion method using glucose as fuel. Based on the XRD, EDS, TEM, and XPS analysis results, we have proved ZnO formation on the surface of the  $\text{LiMn}_2\text{O}_4$  particles. Compared to the pristine  $\text{LiMn}_2\text{O}_4$ , the 2 wt% ZnO-coated  $\text{LiMn}_2\text{O}_4$  sample as a cathode for LIBs exhibited a higher capacity retention of 84.1 % after 500 cycles at 0.5 C and a better rate capacity, still delivering 79.1 mAh  $\text{g}^{-1}$  at 5 C. The improved performance of the surface-coated sample is because the ZnO coating on the surface of  $\text{LiMn}_2\text{O}_4$  can effectively minimize electrochemical polarization and charge transfer resistance during charge-discharge cycling. The XRD results of the 2 wt% ZnO-coated  $\text{LiMn}_2\text{O}_4$  material after 500 cycles revealed that ZnO coating improves the stability of the spinel structure, making lithium ions effectively diffuse in the electrode material. ZnO coating improves the electrochemical performances of  $\text{LiMn}_2\text{O}_4$  comparing with the pristine sample in terms of cycling and rate capability.

**Acknowledgments** The authors acknowledge the financial support from the National Natural Science Foundation of China (51262031, 51462036), Program for Innovative Research Team (in Science and Technology) in the University of Yunnan Province (2011UY09), Yunnan Provincial Innovation Team (2011HC008), and Innovation Program of Yunnan Minzu University (2015YJXCXZ21, 20, 22, 24, 2015TX011,019).

## References

- Vidu R, Stroeve P (2004) Improvement of the thermal stability of Li-ion batteries by polymer coating of  $\text{LiMn}_2\text{O}_4$ . *Ind Eng Chem Res* 43:3314–3324
- Chung DW, Balke N, Kalinin SV, Garcia RE (2011) Virtual electrochemical strain microscopy of polycrystalline  $\text{LiCoO}_2$  films. *J Electrochem Soc* 158:A1083–A1089
- Amatucci G, Tarascon JM (2002) Optimization of insertion compounds such as  $\text{LiMn}_2\text{O}_4$  for Li-ion batteries. *J Electrochem Soc* 149:K31–K46
- He XM, Li JJ, Cai Y, Wang YW, Ying JR, Jiang CY, Wan CR (2005) Preparation of spherical spinel  $\text{LiMn}_2\text{O}_4$  cathode material for lithium ion batteries. *J Solid State Electrochem* 9:438–444
- Jang DH, Oh SM (1998) Effects of carbon additives on spinel dissolution and capacity losses in 4 V  $\text{Li/Li}_x\text{Mn}_2\text{O}_4$  rechargeable cells. *Electrochim Acta* 43:1023–1029
- Aoshima T, Okahara K, Kiyohara C, Shizuka K (2001) Mechanisms of manganese spinels dissolution and capacity fade at high temperature. *J Power Sources* 97-98:377–380
- Yamada A, Tanaka M, Tanaka K, Sekai K (1999) Jahn-Teller instability in spinel Li-Mn-O. *J Power Sources* 81-82:73–78
- Gao Y, Dahn JR (1996) Correlation between the growth of the 3.3 V discharge plateau and capacity fading in  $\text{Li}_{1+x}\text{Mn}_{2-x}\text{O}_4$  materials. *Solid State Ionics* 84:33–40
- Yao JH, Shen CQ, Zhang PJ, Gregory DH, Wang LB (2013) Surface coating of  $\text{LiMn}_2\text{O}_4$  spinel via in situ hydrolysis route: effect of the solution. *Ionics* 19:739–745
- Liu DQ, Liu XQ, He ZZ (2007) Surface modification by ZnO coating for improving the elevated temperature performance of  $\text{LiMn}_2\text{O}_4$ . *J Alloys Compd* 436:387–391
- Ha HW, Yun NJ, Kim K (2007) Improvement of electrochemical stability of  $\text{LiMn}_2\text{O}_4$  by  $\text{CeO}_2$  coating for lithium-ion batteries. *Electrochim Acta* 52:3236–3241
- Zhao S, Chang QJ, Jiang K, Bai Y, Yang YQ, Zhang WF (2013) Performance improvement of spinel  $\text{LiMn}_2\text{O}_4$  cathode material by  $\text{LaF}_3$  surface modification. *Solid State Ionics* 253:1–7
- Shang YS, Liu JL, Huang T, Yu AS (2013) Effect of heat treatment on the structure and electrochemical performance of  $\text{FePO}_4$  coated spinel  $\text{LiMn}_2\text{O}_4$ . *Electrochim Acta* 113:248–255
- Zhao JQ, Wang Y (2013) Surface modifications of Li-ion battery electrodes with various ultrathin amphoteric oxide coatings for enhanced cycleability. *J Solid State Electrochem* 17:1049–1058
- Tu J, Zhao XB, Cao GS, Zhu TJ, Zhung DG, Tu JP (2006) Electrochemical performance of surface-modified  $\text{LiMn}_2\text{O}_4$  prepared by a melting impregnation method. *J Mater Sci Technol* 22:433–436
- Qing CB, Bai Y, Yang JM, Zhang WF (2011) Enhanced cycling stability of  $\text{LiMn}_2\text{O}_4$  cathode by amorphous  $\text{FePO}_4$  coating. *Electrochim Acta* 56:6612–6618
- Cho MY, Roh KC, Park SM, Lee JW (2011) Effects of  $\text{CeO}_2$  coating uniformity on high temperature cycle life performance of  $\text{LiMn}_2\text{O}_4$ . *Mater Lett* 65:2011–2014
- Arumugam D, Kalaigan GP (2008) Synthesis and electrochemical characterizations of nano- $\text{SiO}_2$ -coated  $\text{LiMn}_2\text{O}_4$  cathode materials for rechargeable lithium batteries. *J Electroanal Chem* 624:197–204
- Tu J, Zhao XB, Cao GS, Zhung DG, Zhu TJ, Tu JP (2006) Enhanced cycling stability of  $\text{LiMn}_2\text{O}_4$  by surface modification with melting impregnation method. *Electrochim Acta* 51:6456–6462
- Zhao JQ, Wang Y (2012) Ultrathin surface coatings for improved electrochemical performance of lithium ion battery electrodes at elevated temperature. *J Phys Chem C* 116:11867–11876
- Hu YM, Yao J, Zhao Z, Zhu MY, Li Y, Jin HM, Zhao HJ, Wang JZ (2013) ZnO-doped  $\text{LiFePO}_4$  cathode material for lithium-ion battery fabricated by hydrothermal method. *Mater Chem Phys* 141:835–841
- Singhala R, Tomarb MS, Burgos JG, Katiyara RS (2008) Electrochemical performance of ZnO-coated  $\text{LiMn}_{1.5}\text{Ni}_{0.5}\text{O}_4$  cathode material. *J Power Sources* 183:334–338
- Kong JZ, Ren C, Tai GA, Zhang X, Li AD, Wu D, Li H, Zhou F (2014) Ultrathin ZnO coating for improved electrochemical performance of  $\text{LiNi}_{0.5}\text{Co}_{0.2}\text{Mn}_{0.3}\text{O}_2$  cathode material. *J Power Sources* 266:433–439
- Tu J, Zhao XB, Xie J, Cao GS, Zhung DG, Zhu TJ, Tu JP (2007) Enhanced low voltage cycling stability of  $\text{LiMn}_2\text{O}_4$  cathode by ZnO coating for lithium ion batteries. *J Alloys Compd* 432:313–317
- Liu HW, Cheng CX, Hu ZQ, Zhang KL (2007) The effect of ZnO coating on  $\text{LiMn}_2\text{O}_4$  cycle life in high temperature for lithium secondary batteries. *Mater Chem Phys* 101:276–279



26. Xia Y, Huang M, Chen MM, Zhang YJ, Guo JM (2013) Modification of the solution flameless combustion synthesis of spinel  $\text{LiMn}_2\text{O}_4$  by nitric acid. *Asian J Chem* 25:1917–1920
27. Manthiram A, Murugan AV, Sarkar A, Muraliganth T (2008) Nanostructured electrode materials for electrochemical energy storage and conversion. *Energy Environ Sci* 1:621–638
28. Arumugama D, Kalaignana GP, VEDIAPPAN K, Lee CW (2010) Synthesis and electrochemical characterizations of nano-scaled Zn doped  $\text{LiMn}_2\text{O}_4$  cathode materials for rechargeable lithium batteries. *Electrochim Acta* 55:8439–8444
29. Umar A, Kim SH, Lee YS, Nahm KS, Hahn YB (2005) Catalyst-free large-quantity synthesis of ZnO nanorods by a vapor-solid growth mechanism: structural and optical properties. *J Cryst Growth* 282:131–136
30. Umar A, Hahn YB (2006) ZnO nanosheet networks and hexagonal nanodisks grown on silicon substrate: growth mechanism and structural and optical properties. *Nanotechnology* 17:2174–2180
31. Wahab R, Ansari SG, Kim YS, Seo HK, Kim GS, Khang G, Shin HS (2007) Low temperature solution synthesis and characterization of ZnO nano-flowers. *Mater Res Bull* 42:1640–1648
32. Zhang XS, Xu YL, Zhang H, Zhao CJ, Qian XZ (2014) Structure and cycle stability of  $\text{SrHPO}_4$ -coated  $\text{LiMn}_2\text{O}_4$  cathode materials for lithium-ion batteries. *Electrochim Acta* 145:201–208
33. Rui XH, Sim DH, Xu C, Liu WL, Tan HT, Wong KM, Hng HH, Lim TM, Yan QY (2012) One-pot synthesis of carbon-coated  $\text{VO}_2(\text{B})$  nanobelts for high-rate lithium storage. *RSC Adv* 2: 1174–1180
34. Liu ZL, Wang HB, Fang L, Lee JY, Gan LM (2002) Improving the high-temperature performance of  $\text{LiMn}_2\text{O}_4$  spinel by micro-emulsion coating of  $\text{LiCoO}_2$ . *J Power Sources* 104: 101–107
35. Zhao HY, Li F, Liu XQ, Cheng C, Zhang Z, Wu Y, Xiong WQ, Chen B (2015) Effects of equimolar Mg (II) and Si (IV) co-doping on the electrochemical properties of spinel  $\text{LiMn}_{2-2x}\text{Mg}_x\text{Si}_x\text{O}_4$  prepared by citric acid assisted sol-gel method. *Electrochim Acta* 151: 263–269
36. Mohamedi M, Takahashi D, Uchiyama T, Itoh T, Nishizawa M, Uchida I (2001) Explicit analysis of impedance spectra related to thin films of spinel  $\text{LiMn}_2\text{O}_4$ . *J Power Sources* 93:93–103
37. Jiang RY, Cui CY, Ma HY, Ma HF, Chen T (2015) Study on the enhanced electrochemical performance of  $\text{LiMn}_2\text{O}_4$  cathode material at 55 °C by the nano Ag-coating. *J Electroanal Chem* 744:69–76
38. Xiong LL, Xu YL, Tao T, Goodenough JB (2012) Synthesis and electrochemical characterization of multi-cations doped spinel  $\text{LiMn}_2\text{O}_4$  used for lithium ion batteries. *J Power Sources* 199: 214–219
39. Ni JF, Zhou HH, Chen JT, Zhang XX (2008) Improved electrochemical performance of layered  $\text{LiNi}_{0.4}\text{Co}_{0.2}\text{Mn}_{0.4}\text{O}_2$  via  $\text{Li}_2\text{ZrO}_3$  coating. *Electrochim Acta* 53:3075–3083
40. Woo SU, Yoon CS, Amine K, Belharouak I, Sun YK (2007) Significant improvement of electrochemical performance of  $\text{AlF}_3$ -coated  $\text{Li}[\text{Ni}_{0.8}\text{Co}_{0.1}\text{Mn}_{0.1}]\text{O}_2$  cathode materials. *J Electrochem Soc* 154:A1005–A1009